COMPDYN 2011
III ECCOMAS Thematic Conference on
Computational Methods in Structural Dynamics and Earthquake Engineering
M. Papadrakakis, M. Fragiadakis, V. Plevris (eds.)
Corfu, Greece, 25–28 May 2011

SEISMIC RESPONSE ESTIMATION OF A NUCLEAR POWER PLANT STRUCTURE CONSIDERING NEARBY FAULT BASED ON A MULTISCALE APPROACH

Pher Errol B. Quinay[1], Tsuyoshi Ichimura[2], and Muneo Hori[2]

[1] Earthquake Research Institute, University of Tokyo
1-1-1 Yayoi, Bunkyo-ku, Tokyo 113-0032, Japan
equinay2@eri.u-tokyo.ac.jp

[2] Earthquake Research Institute, University of Tokyo
1-1-1 Yayoi, Bunkyo-ku, Tokyo 113-0032, Japan
{ ichimura, hori }@ eri.u-tokyo.ac.jp

Keywords: Fault-structure system, multiscale, nuclear power plant.

Abstract. *An approach to estimate the response of a model of nuclear power plant (NPP) that includes the rupture of a nearby fault using a multiscale approach is demonstrated. The conceptual model is the fault-structure system: a system that models the 3D fault rupture process, wave propagation through the irregular crust structure, effect of local geologic setting at the NPP location, and response of NPP structure. A multiscale method, called Macro-Micro Analysis is employed, which resulted to reduction in computation cost. A reproduction of a recent earthquake event in Kanto region is performed to check the earthquake wave propagation and compare the resulting synthetic seismogram to the recorded seismogram in an observation station. A scenario earthquake simulation is then conducted and the response of NPP under this scenario is obtained. Results have revealed irregular structure deformation caused by the varying phase and amplitude characteristics of the input wave caused by the scenario earthquake.*

1 INTRODUCTION

Estimating the seismic response of nuclear power plant (NPP) structures poses a big computational challenge because of the need to account for the geologic settings of the site. Past earthquakes generated from the nearby fault have shown that NPP is vulnerable to large deformations and large amplitude acceleration. To obtain a reliable structure response, the components of seismic analysis should be modeled with high resolution. It is known that the input ground motion is affected by the following factors: fault-rupture process, irregular crust structure, soft basin layer, and site-specific conditions such as topography and nature of soil at site vicinity. Thus, aiming to model all processes related to these factors is desirable, but as mentioned, to satisfy the high resolution modeling, a large computational environment is needed.

In computation, the above problem is called fault-structure system (FSS). FSS is a conceptual model that includes modeling all the significant processes in the problem of seismic wave propagation and seismic response of structure. The aim of this approach is to account for the three-dimensional (3D) variability of each process (as examples: radiation of seismic waves from the source, response of structure with geometrical irregularities). To reduce the heavy demand for computational resources, a multiscale-based method, called the Macro-Micro Analysis (MMA) has been proposed by Ichimura and Hori [1]. MMA decomposes the FSS problem into two scales and refines the solution as each scale is solved. It is noted that MMA's applicability has been earlier demonstrated on the analysis of large-scale underground structure [1]. This study extends the applicability of this multiscale approach to NPP seismic response estimation.

2 METHODOLOGY

2.1 Multiscale Approach and the Macro-Micro Analysis

It can be observed that two length scales are being considered when solving the FSS – the geologic-length scale (for seismic wave propagation) and engineering-length scale (for seismic structural response). In these two scales, the spatial dimensions would vary from about 10^5 meters for the domain size for seismic wave propagation to about 10^{-1} meters for the structure mesh to obtain high resolution output. Thus, if all components are simultaneously solved, the resulting computation cost can be very high which may not be practical to run in the present computational environment. MMA derives the mathematical basis for performing a multiscale approach applicable to these two scales that reduces the cost of solving the FSS.

The MMA applies the perturbation technique to the elastodynamic problem,

$$d_i\left(c_{ijkl} d_l(u_k)\right) - \rho \ddot{u}_j = 0 \tag{1}$$

where c_{ijkl}, ρ, u_k, d_i, $(\dot{})$ are the component of elasticity tensor, mass density, displacement component, partial differentiation, and temporal differentiation, respectively.

The singular perturbation expansion method [2] expands the solution u_k of the wave equation as,

$$u_k \approx u_k^{(0)} + \varepsilon u_k^{(1)} + \ldots \tag{2}$$

where $u^{(0)}$ is solution at low resolution, $u^{(1)}$ is solution at high resolution, and $\varepsilon = X_i/x_i$ is a very small parameter (<<1) that relates the slow spatial variable, X to fast-changing variable, x.

Using Equation (2) on Equation (1) results to two equations that first, computes the solution in the domain of the slow spatial variable, and then refines this solution using the properties near the structure:

$$D_i\left(C_{ijkl} D_l u_k^{(0)}\right) - R\ddot{u}_j^{(0)} = 0 \tag{3}$$

$$d_i\left(c_{ijkl}\left(d_l u_k^{(1)} + d_l u_k^{(0)}\right)\right) - \rho\left(\ddot{u}_j^{(1)} + \ddot{u}_j^{(0)}\right) = 0 \tag{4}$$

where D_i is differentiation with respect to X_i , R is the effective density, and C_{ijkl} is the equivalent elasticity tensor in the domain of the slow spatial variable. Equation (3) and Equation (4) are called the Macro and Micro analysis of the MMA, respectively. Figure 1 shows the schematic of the MMA in relation to FSS. The details of derivation of these equations can be found in Ichimura and Hori [1, 3]

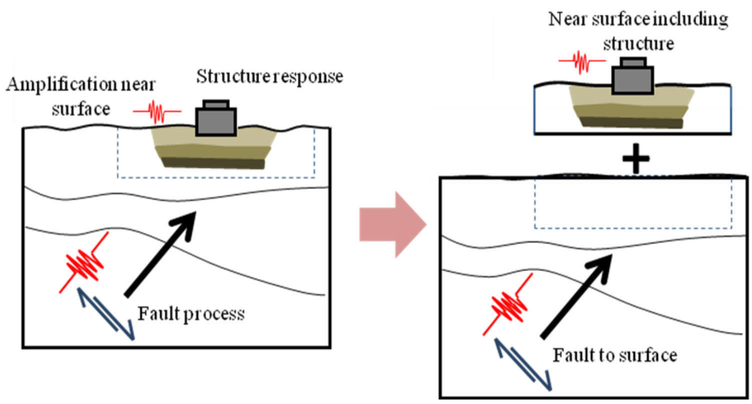

Figure 1: Decomposition of FSS (left) to Macro Analysis (bottom right) and Micro Analysis (top right).

2.2 Computing the Macro and Micro Analysis

In MMA, modeling the earthquake wave generation and propagation (Macro analysis) includes accounting for the fault-rupture settings and the properties of irregular crust structure and basin velocity structures. Given Equation (3), the spatial component is discretized using the Galerkin method, and the time integration method used is Newmark-β (β=1/4) method. A Rayleigh damping term is added to account for material (layer) damping:

$$\left(\mathbf{K}+\frac{2}{\Delta t}\mathbf{C}+\frac{4}{\Delta t^2}\mathbf{M}\right)\mathbf{u}^{n+1}=\left(\frac{2}{\Delta t}\mathbf{C}+\frac{4}{\Delta t^2}\mathbf{M}\right)\mathbf{u}^{n}+\left(\mathbf{C}+\frac{4}{\Delta t}\mathbf{M}\right)\mathbf{v}^{n}+\mathbf{M}\mathbf{a}^{n}+\mathbf{f}^{n} \quad (5)$$

where **K**, **C**, **M**, **u**, **v**, **a**, **f**, *n*, Δt are stiffness matrix, Rayleigh damping matrix, mass matrix, displacement vector, velocity vector, acceleration vector, external force vector, temporal counter, and time step size, respectively.

In the Macro analysis simulation, the response at the nodes that are shared with the boundary of the Micro model is stored as input boundary condition for the Micro analysis. The Micro model includes the site-specific conditions such as soft soil layers that will add to the coarse solution of Macro analysis as refinement. The Micro analysis is carried out following Equation (4). Discretization in space using the Galerkin method and in time using Newmark-β (β=1/4) method, results to an equation similar to Equation (5) without the external force term.

In Macro and Micro modeling, hybrid-grid FEM (HyFEM) [3] is implemented to reduce memory usage and computation time. HyFEM uses the background cell, voxel [4], and octree technique [5] for finite element mesh arrangement and for the analysis, element-by-element method [6] and preconditioned conjugate gradient method (PCG) are implemented. For the details of the Macro and Micro analysis and implementation of the computation techniques, the reader is referred to the following related papers: [1, 3, 7, 8].

3 APPLICATION EXAMPLE

3.1 Reproduction of observed ground motion

The Macro analysis code is validated for application to earthquake simulation by conducting a reproduction of an observed earthquake event. An earthquake that occurred on May 9, 2010 in Tokyo is selected. For the simulation, a region that includes a small part of Kanto region is selected, as shown in Figure 2. The crust layer information derived by Tanaka et al. [9] for this selected region is given on Table 1. The earthquake information (fault parameter) were taken from F-NET [10], and the recorded seismograms on seismic station TKY 021 (about 14.4 km from the epicenter) were taken from K-NET [11]. This earthquake is modeled as a double-couple point source with settings as given in Table 2. In this simulation, the target accuracy is 0.5 Hz. Time step size is 0.01 seconds and total time duration is 40.96 seconds. The criterion for spatial discretization is 10 elements for one wavelength (minimum element size is 100 m). The iterative solver is PCG method with convergence criteria of $1 \mathrm{x} 10^{-6}$.

Layer	P-wave velocity (m/s)	S-wave velocity (m/s)	Density (kg/m^3)	Quality factor
1	1850	500	1950	60
2	2560	1000	2150	150
3	3200	1700	2300	200
4	5800	3360	2700	500
5	6600	3700	2800	600
6	8040	4480	4400	800

Table 1. Layer material properties used in reproduction of observed earthquake [9].

Date	2010/05/09
Latitude	35.6757 N
Longitude	139.6613 E
Depth	26.73 km
Source time function	$M_o(2t^2/T_o^2)\ \ 0 \leq t \leq T_o/2$
	$M_o(1-2(t-T_o)^2/T_o^2)\ \ T_o/2 \leq t \leq T_o$
	$M_o\ \ \ t \geq T_o$
Magnitude	Mw = 3.8
Strike, Dip, Rake	253^o, 17^o, 39^o
Rise time, To	0.18 sec

Table 2. Observed earthquake properties [11].

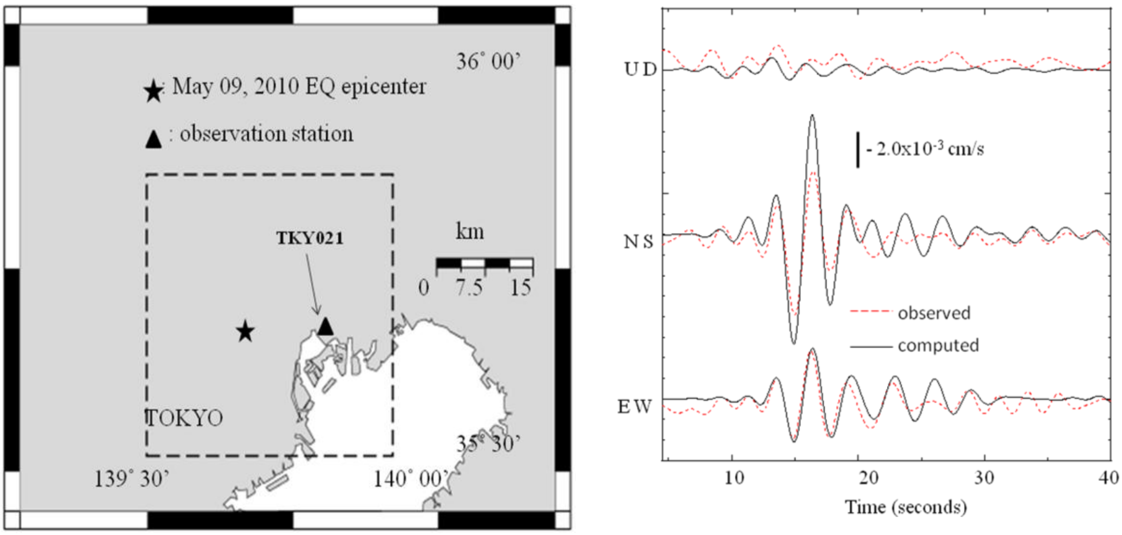

Figure 2: Reproduction of observed earthquake: Left: simulation region and location of epicenter and observation point; Right: comparison of observed and synthetic seismograms at observation station TKY021 (bandpass-filtered [0.0Hz-1.0Hz]).

Figure 2 (right) shows the comparison between the observed and computed (synthetic) seismograms. The comparison shows both agreements and disagreement in amplitude and wave phases at different points, wherein the disagreements can be attributed to the uncertainty in the crust structure data (verified at less than 0.5Hz) and earthquake parameters (moment tensors were derived from inversion analyses using horizontal layered velocity structure [10]). Nevertheless, the results validate the application of Macro analysis code for earthquake wave propagation simulation and for estimating the input boundary condition to the Micro analysis.

3.2 Scenario earthquake and response estimation of NPP

In this section, a scenario earthquake simulation is conducted to perform the complete Macro-Micro Analysis for NPP. For this scenario earthquake, several of the fault parameters are based from the CDPC report for East-Central Tokyo Earthquake Scenario [12] (fault dip and rake, fault rupture speed and fault depth). The fictitious problem setting (as shown in Figure 3) is that the position of the NPP is 13.0 km from the epicenter of a reverse fault close to the surface. The scenario is generated from rupture of a fault plane (modeled as a sequential rupture of points in the fault plane) of about 1.8 km x 1.8 km in dimensions that dips at 45^0 from the horizontal plane (see Figure 3). The depth of the top portion of the fault is about 6 km and rupture propagation speed from the hypocenter (at the depth of 7.2 km) is 2.5 km/s. The details of the point source settings are shown on Table 3.

Hypocenter depth	7.20 km
Rupture speed	2.5 km/s
Source time function	$M_o(2t^2/T_o^2)$ $0 \le t \le T_o/2$
	$M_o(1-2(t-T_o)^2/T_o^2)$ $T_o/2 \le t \le T_o$
	M_o $t \ge T_o$
Magnitude	$M_W = 5.3$
Strike, Dip, Rake	30^o, 45^o, 90^o
Rise time, To	0.216 sec

Table 3. Scenario earthquake point source setting

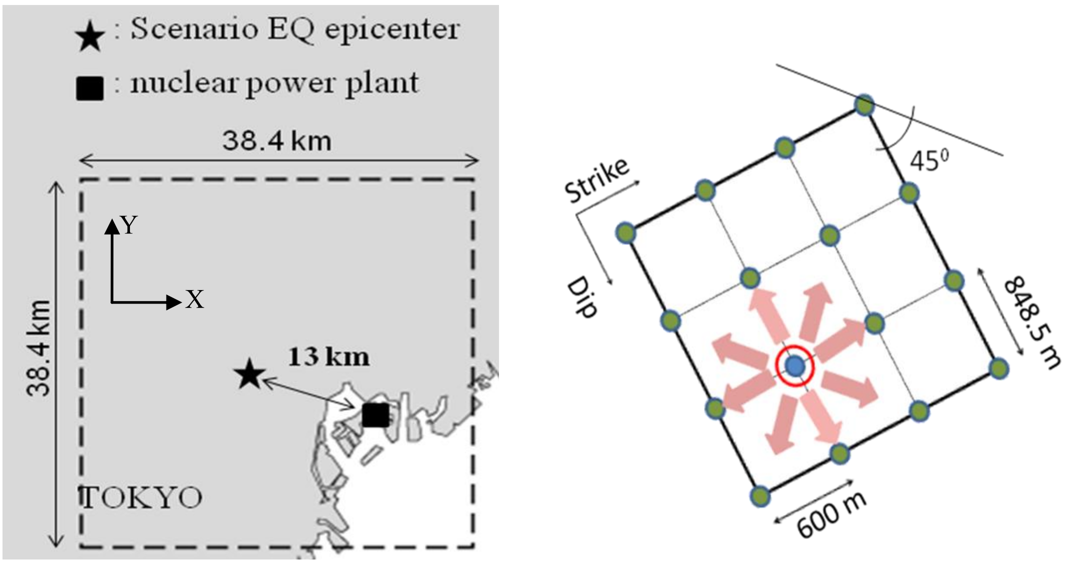

Figure 3: Fictitious problem settings for the scenario earthquake simulation. Left: The relative location of the fault-plane epicenter and the NPP; Right: The fault-plane showing the point sources (in green) that have varied rupture starting time. Hypocenter is encircled in red. Settings of each point source are given on Table 3.

The same model domain and crust layer properties as 3.1 are used. The target accuracy is set at 0.5 Hz. The time increment is 0.01 seconds and total time step is 2048. Criterion for spatial discretization is ten (10) elements for one wavelength (minimum element size is 100 m). The iterative solver is PCG method with convergence criteria of $1x10^{-6}$. Figure 4 shows the Micro model derived from the Macro model (with location of NPP embedded on engineered fill) and the configuration of the NPP meshed model. The material properties of the NPP and engineered-fill are given on Table 4.

Material	P-wave velocity (m/s)	S-wave velocity (m/s)	Density (kg/m3)	Quality factor
Engineered fill	1500	400	1600	50
NPP	3373	2127	2500	200

Table 4. Material properties

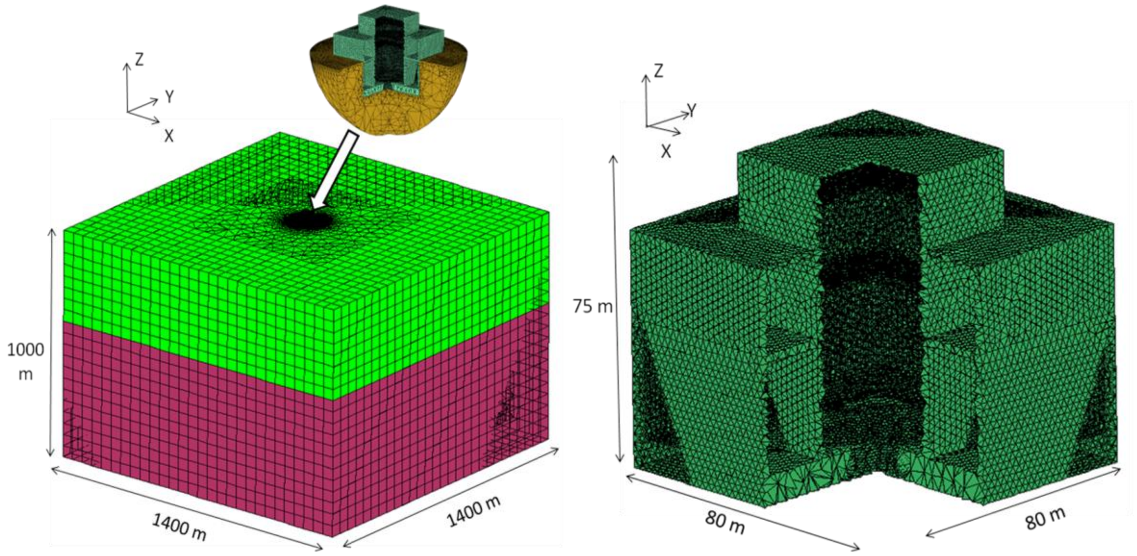

Figure 4: Micro analysis FEM models. Left: the micro model includes two crust layers which are derived from the Macro Analysis model. The location of NPP partially-embedded in an engineered-fill is located at the center of the Micro model; Right: The meshed NPP model and dimensions. The embedded portion is 36.0m from the bottom.

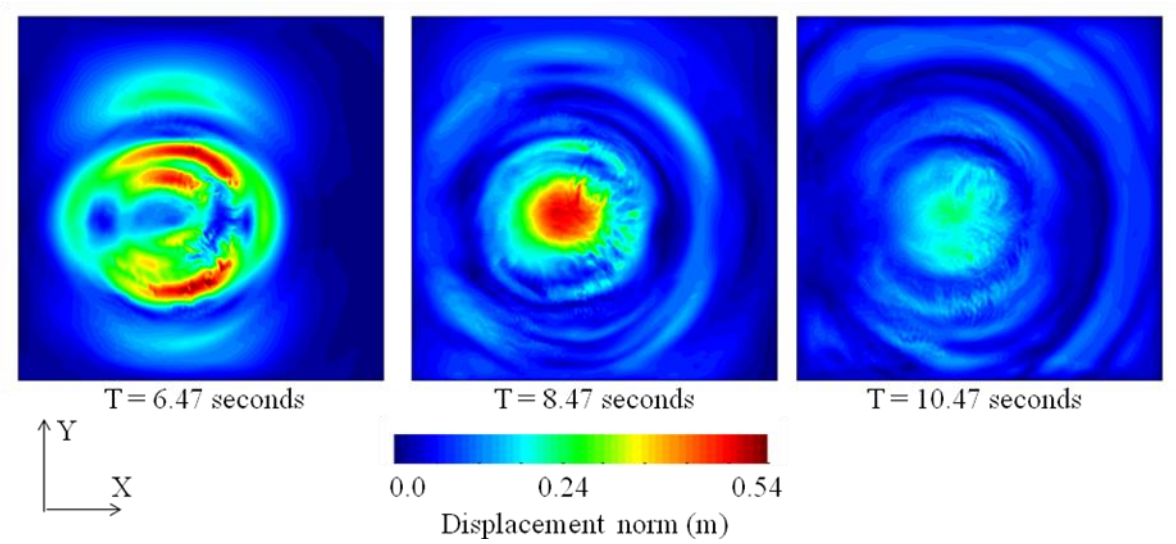

Figure 5: Snapshots of simulation result at surface: displacement norm. The wavefield is made complicated by the effect of the earthquake source, irregular crust structure, and surface topography.

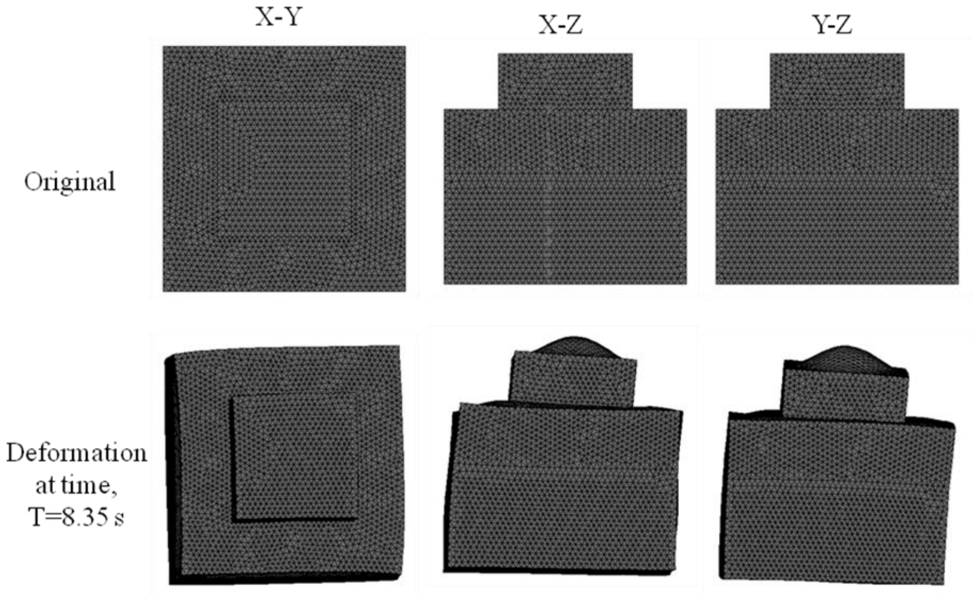

Figure 6: NPP structure deformation (x1500) at time, T = 8.47 seconds. Shown are deformations viewed at three orthogonal directions. Both lateral and vertical deformations are significant because of the effect of configuration of fault plane and direction of rupture.

Figure 5 shows snapshots of the waves at different time intervals as outputted by the Macro Analysis. The corresponding structure response at a given time, as outputted by the Micro Analysis is shown on Figure 6.

Implementing the FSS for estimating the seismic response of NPP from a rupture of a nearby fault is an advantage because the three-dimensional variation of the input wave can be modeled. As shown in Figure 6, the deformation of the NPP varies on all three orthogonal views, evident that the input wave varies in amplitude and phase characteristics in all its spatial components. For an actual NPP, which is geometrically-irregular, the response can be more complicated, and modeling by FSS can aid in identifying the critical locations of the NPP based on the scenario earthquake.

In solving the FSS in a multiscale manner, analysis in geologic- and engineering-length scales are solved efficiently, leading to reduction in computation cost. Thus this methodology would allow for simulations aiming for higher target frequency, which will improve the seismic response estimation of NPP. Given the results presented here, FSS analysis is now being studied for extension to fracture analysis of NPP structures. Moreover, to further reduce the computation time in modeling and analysis, shared and distributed memory parallelization is presently being implemented to the MMA codes.

4 CONCLUSION

An approach to estimate the response of NPP that includes the rupture of a nearby fault using a multiscale approach is presented. This approach, called the FSS, models the important processes related to earthquake wave propagation and seismic response of NPP structure. A multiscale method, called Macro-Micro Analysis is used which resulted to reduction in computation cost. A reproduction of a recent earthquake event in Kanto region is performed to check the earthquake wave propagation and compare the resulting synthetic seismogram to the recorded seismogram in an observation station. A scenario earthquake is then conducted and the response of NPP under this scenario is obtained. Results have shown irregular structure deformation caused by the varying input wave characteristics of the scenario earthquake. These results emphasize the importance of three-dimensional modeling of different components of earthquake wave propagation and structure response for reliable estimation of future strong ground motions.

Acknowledgement

The authors acknowledge the support from the CREST project and Japan Atomic Energy Agency (JAEA).

REFERENCES

[1] T. Ichimura, M. Hori, M., Structural seismic response analysis based on multiscale approach of computing fault-structure system, *Earthquake Engineering and Structural Dynamics*, 38, 439-455, 2009.

[2] D. R. Smith, *Singular Perturbation Theory, An Introduction with Applications*, Cambridge University Press: Cambridge, 1985.

[3] T. Ichimura, M. Hori, J. Bielak, J., A hybrid multiresolution meshing technique for Finite Element three-dimensional earthquake ground motion modeling in basins including topography," *Geophysical Journal International*. 177, 1221-1232, 2009.

[4] K. Koketsu, H. Fujiwara, Y. Ikegami, Finite Element simulation of seismic ground motion with a voxel mesh, *Pure and Applied Geophysics*, Vol. 161, pp.2183-2198, 2004.

[5] J. Bielak, O. Ghattas, E.J. Kim, Parallel Octree-based Finite Element Method for large-scale earthquake ground motion simulation, *Computer Modeling in Engineering and Sciences*, Vol. 10, 99-112, 2005.

[6] J. M. Winget, and T. J. R. Hughes, Solution algorithms for nonlinear transient heat conduction analysis employing element-by-element iterative strategies," *Computer Methods in Applied Mechanics and Engineering*., 52, 711-815, 1985.

[7] T. Ichimura, M. Hori, Macro-Micro Analysis method for wave propagation in stochastic media, *Earthquake Engineering and Structural Dynamics*, 35, 419-432, 2006.

[8] T. Ichimura, M. Hori, H. Kuwamoto, Earthquake motion simulation with multiscale Finite-Element Analysis on hybrid grid," *Bulletin of Seismological Society of America*, Vol. 97, No. 4, 1133-1143, 2007.

[9] Y. Tanaka, H. Miyake, K. Koketsu, T. Furumura, T. Hayakawa, T. Baba, H. Suzuki, T. Masuda, The DaiDaiToku integrated model of the velocity structure beneath the Tokyo Metropolitan Area (2)," *Abstracts of the Japan Geoscience Union Meeting*, S116-P014, 2006.

[10] F-net Broadband Seismograph Network, Japan National Research Institute for Earth Science and Disaster Prevention, http://www.fnet.bosai.go.jp/freesia/

[11] K-net Kyoshin Network, Broadband Seismograph Network, Japan National Research Institute for Earth Science and Disaster Prevention, http://www.k-net.bosai.go.jp

[12] Central Disaster Prevention Council (CDPC) (2004), Working Report on Near-field Earthquake beneath Central Tokyo, http://www.bousai.go.jp/jishin/chubou/shutochokka/12/shiryo2-2.pdf (in Japanese).